Electronic Supplementary Material (ESI) for Journal of Materials Chemistry A.

Serpentcactus-like Co-doped $Ni(OH)_2/Ni_3S_2$ hierarchical structure composed of ultrathin nanosheets for efficient asymmetric supercapacitor

Lin Ye,[a] Lijun Zhao,[a,*] Hang Zhang,[a] Ping Zan,[a] Shuai Gen,[a] Wenhui Shi,[a] Bing Han,[b] Haiming Sun,[a] Xijia Yang,[a] and Tianhao Xu[a]

[a]Key Laboratory of Automobile Materials, Ministry of Education and School of Materials Science and Engineering, Jilin University, Changchun, 130022, P. R. China
*E-mail: lijunzhao@jlu.edu.cn
[b]Alan G. MacDiarmid Institute, College of Chemistry, Jilin University, Changchun 130012, P. R. China

Electrochemical Calculations

The specific capacitance (Cs) values of the individual electrode and ASC setup could be easily obtained according to Equation (1):

$$Cs=I\Delta t/(mV) \qquad (1)$$

Where Cs, I, Δt and m are corresponding to the specific capacitance (F g^{-1}), current (A), discharge time (s) and the total active materials mass (g) of individual electrode and ASC, and V represents the entire potential window of individual electrode and ASC.

The matching mass of positive and negative electrodes referring to Equation (2) as follow:

$$m_+/m_-=Cs_-V_-/(Cs_+V_+) \qquad (2)$$

where m_+ and m_- are the active materials mass (g) of positive and negative electrodes, respectively; Cs_+ and Cs_- are the specific capacitance (F g^{-1}) of positive and negative electrodes, respectively; V_+ and V_- are the potential window (V) of specific capacitance of positive and negative electrodes, respectively.

For ASC devices, the energy density (E, W h kg^{-1}) and power density (P, W kg^{-1}) can be available based on Equation (3) and Equation (4):

$$E=1/2CsV^2 \qquad (3)$$

$$P= E/\Delta t \qquad (4)$$

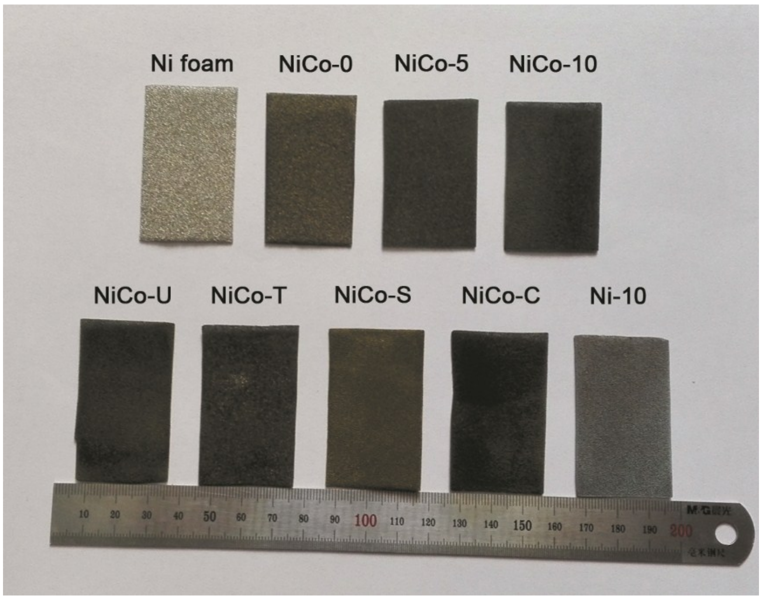

Fig. S1 Photograph of Ni foam, NiCo-0, NiCo-5, NiCo-10, NiCo-U, NiCo-T, NiCo-S，NiCo-C and Ni-10 samples.

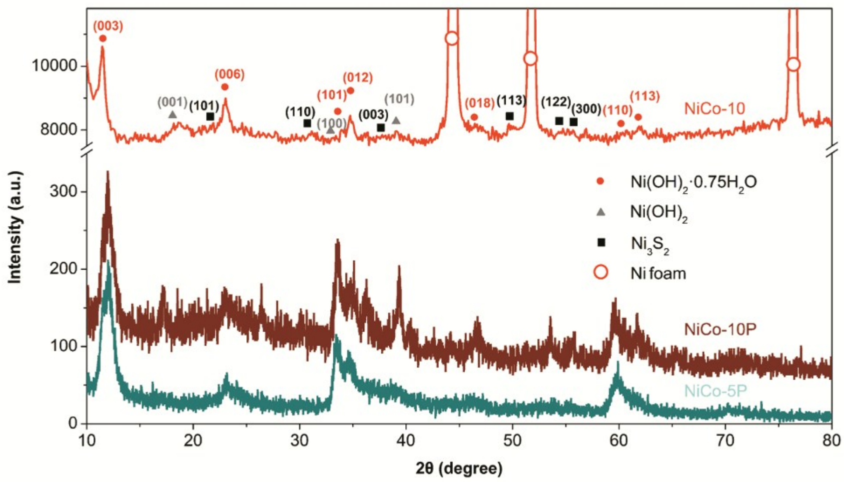

Fig. S2 XRD patterns of NiCo-10, NiCo-5P and NiCo-10P.

In the preparation of NiCo-5 and NiCo-10, extra precipitates could be collected and marked NiCo-5P, NiCo-10P, respectively. Besides, there is little precipitate in the preparation of NiCo-0. Compared with NiCo-10, NiCo-5P and NiCo-10P display sharp peaks and consistent peak positions, furthering confirming the existence of $Ni(OH)_2 \cdot 0.75H_2O$ (JCPDS No. 38-0715), $Ni(OH)_2$ (JCPDS No.14-0117) and Ni_3S_2 (JCPDS No. 44-1418) phases in the as-prepared NiCo-based composites.

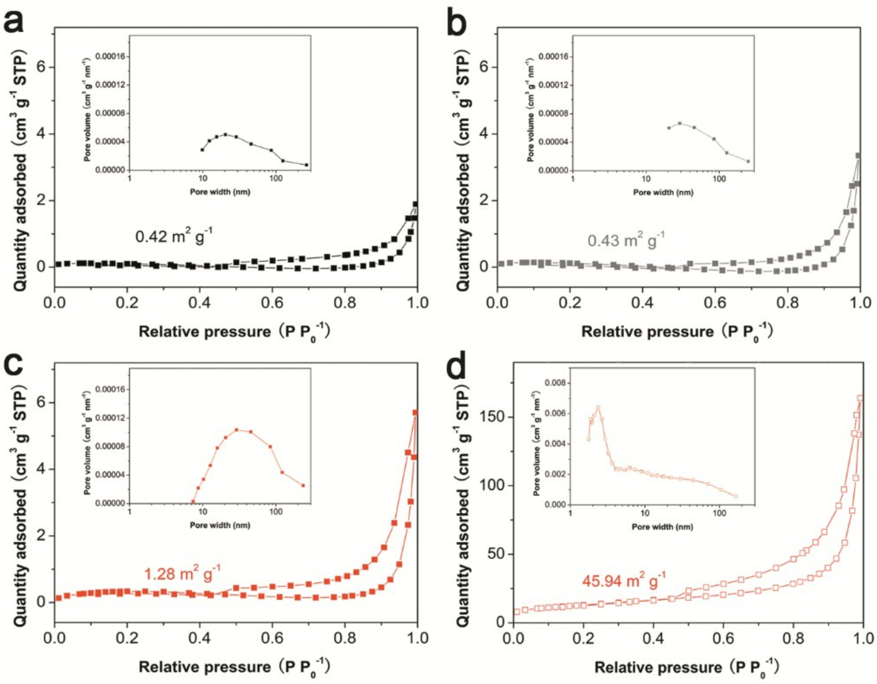

Fig. S3 N_2 adsorption-desorption isotherms and corresponding BJH pore-size distribution curves in their insets: (A) NiCo-0; (B) NiCo-5; (C) NiCo-10; (D) NiCo-10P.

Herein, the specific surface area of NiCo-0, NiCo-5 and NiCo-10 (based on the total mass of samples with 15 cm^2) are 0.42, 0.43 and 1.28 $m^2\ g^{-1}$. Thanks to Ni foams are completely covered with active materials in the NiCo-0, NiCo-5 and NiCo-10 samples, so the Ni foams don't contribute to specific surface area in these samples. According to $BET_{active} = BET_{total}*M_{total}/M_{active}$, the BET values of NiCo-0, NiCo-5 and NiCo-10 are 33.28, 17.11 and 31.63 $m^2\ g^{-1}$, where M_{total} and M_{active} are the mass of active materials and total mass of samples, BET_{active} and BET_{total} are the specific surface area based on M_{total} and M_{active}. Additionally, the NiCo-10P powder possesses a BET values of 45.94 $m^2\ g^{-1}$, also implying a large specific surface area of NiCo-10. Besides, the NiCo-0, NiCo-5, NiCo-10 and NiCo-10P have a broad pore size distribution extending to about 300 nm, and their average pore sizes are 25.2 nm, 36.4 nm, 14.1 nm and 11.0 nm, respectively. The abundant open space provides more sufficient contact area between active materials and electrolyte.

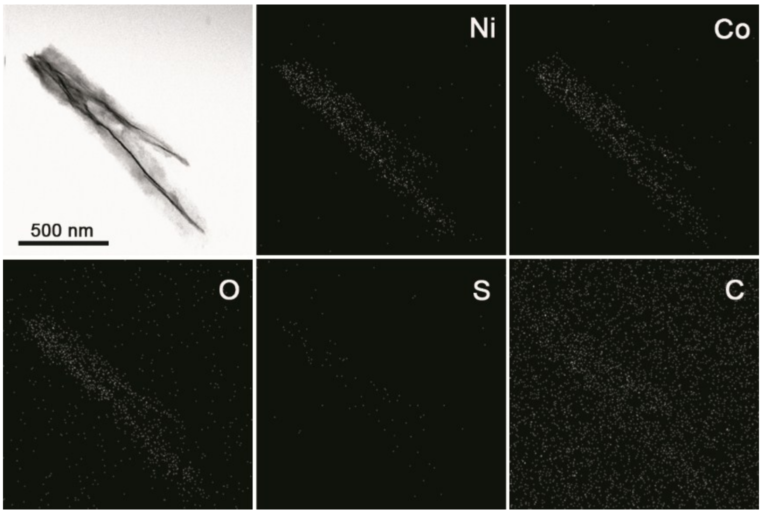

Fig. S4 Elemental mapping of exfoliated 1D SL NiCo-10 structure.

The mapping result in Fig. S4 indicates the uniform distribution of Ni, Co, O, S and C elements.

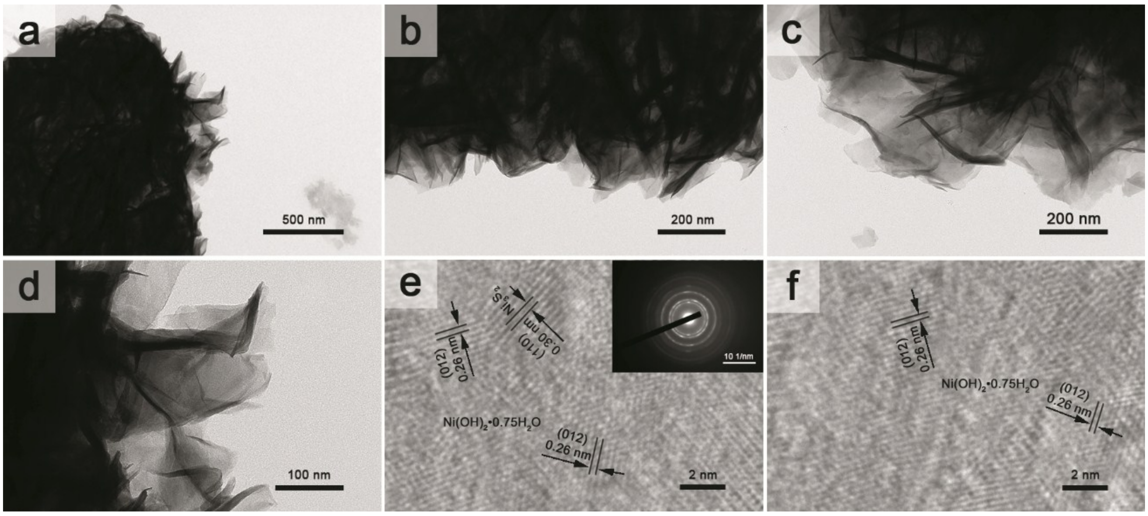

Fig. S5 (a-d) TEM figures of NiCo-0; (e and f) HRTEM figures of NiCo-0. The inset is the SAED pattern of NiCo-0.

After ultrasonication, the lacerated NiCo-0 nanosheets overlap, ripple or wrinkle in order to reduce high surface free energy, which originates from thin structure. The SAED pattern reveals its polycrystalline property.

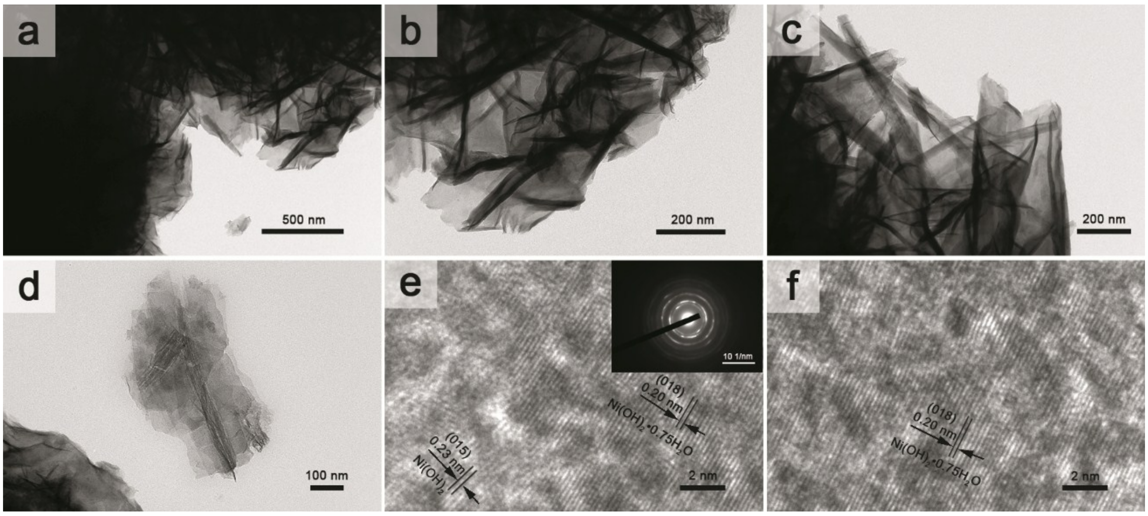

Fig. S6 (a-d) TEM figures of NiCo-5; (e and f) HRTEM figures of NiCo-5. The inset is SAED pattern of NiCo-5.

As shown in Fig. S6, except overlapped, rippled or wrinkled nanosheets, 1D SL structure could be found, indicating the incomplete transformation of 1D SL structure. The SAED pattern also indicates its polycrystalline property.

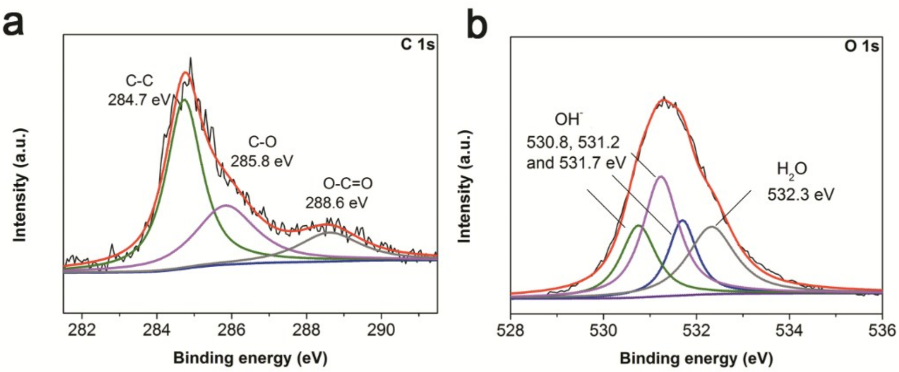

Fig. S7 XPS spectra of NiCo-10: (a) C 1s and (b) O 1s.

In Fig. S7a, the three peaks at 284.7, 285.8 and 288.6 eV attribute to the C-C, C-O and O-C=O bonds, respectively[1, 2] Notably, the dominated C-C results from the CTAB surfactant according to the entire reaction system, indicating CTAB molecules are attached on NiCo-10. In the O 1s region, the presence of peak at 532.3 eV suggests the existence of H_2O in the samples that derived from crystal water and absorbed water in air,[3] while the peaks at 530.8, 531.2 and 531.7 eV are spin–orbit doublet characteristics of OH^- ions combining with nickel or cobalt ions based on XPS manual.

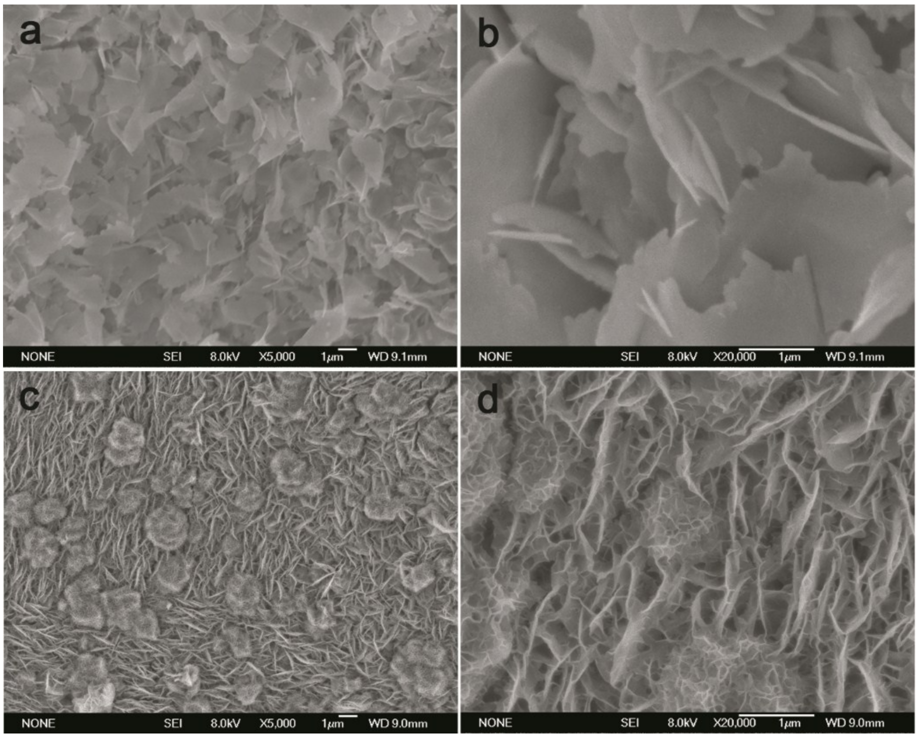

Fig. S8 (a and b) FESEM figures of NiCo-T at various magnifications; (c and d) FESEM figures of NiCo-U at various magnifications.

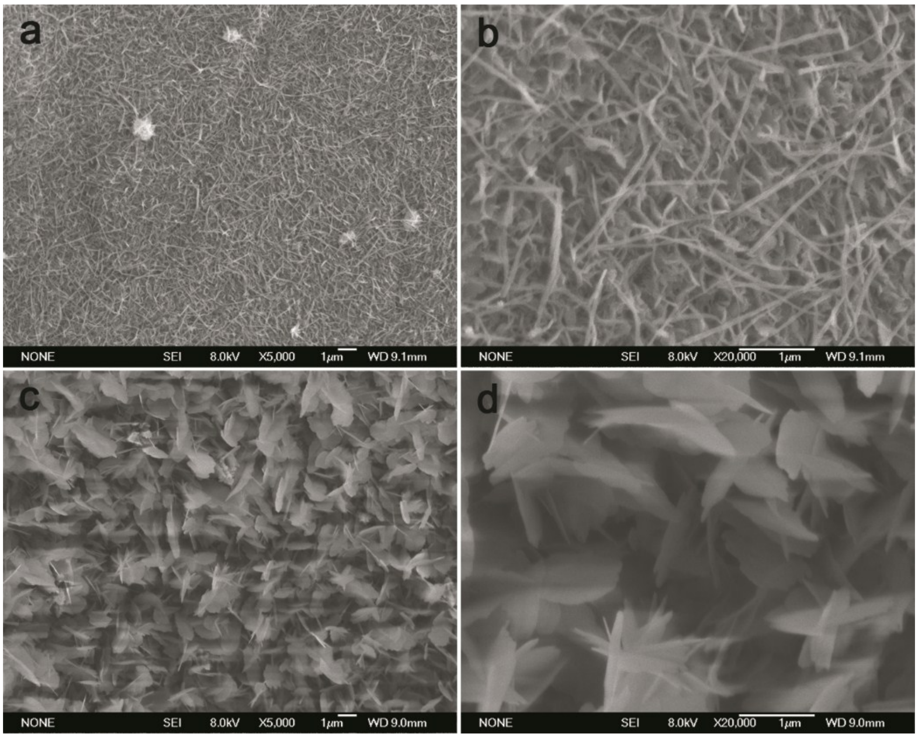

Fig. S9 (a and b) FESEM figures of NiCo-S at various magnifications; (c and d) FESEM figures of NiCo-C at various magnifications.

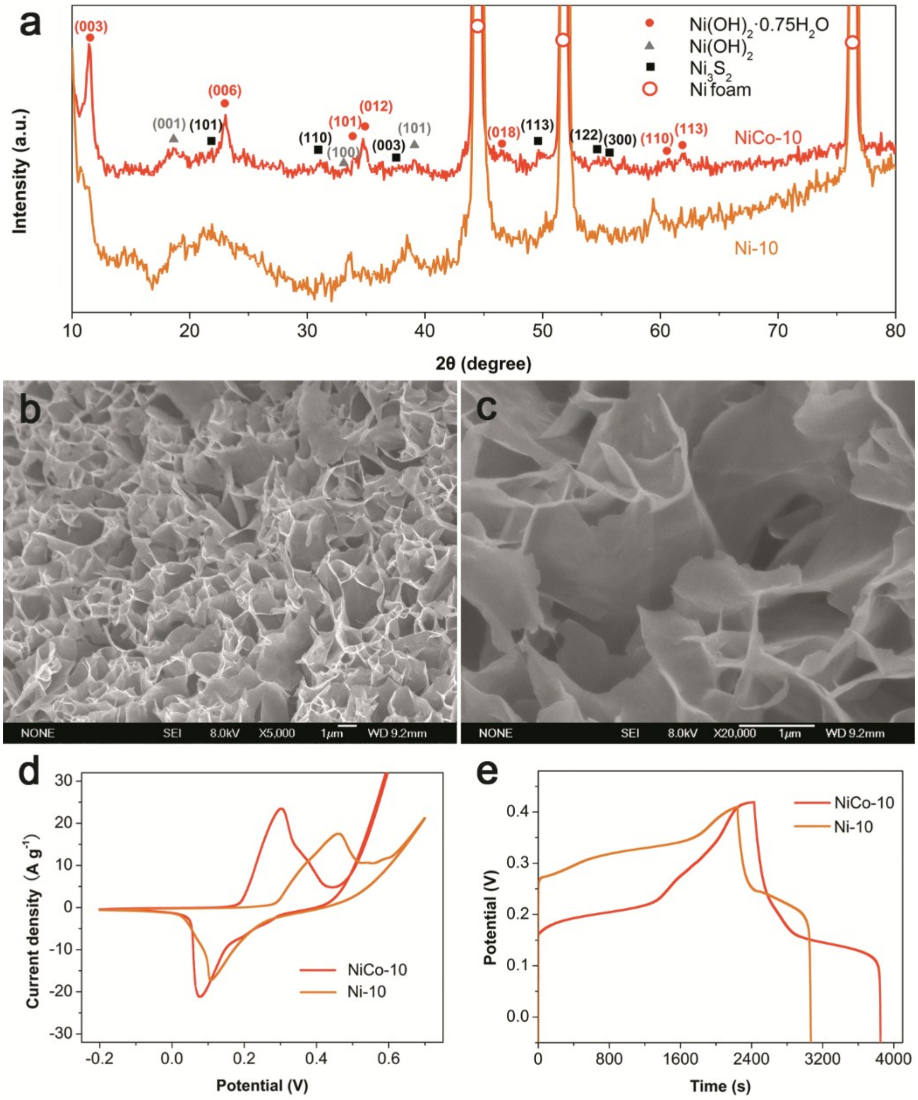

Fig. S10 (a) XRD patterns of NiCo-10 and Ni-10; (b and c) FESEM figures of Ni-10 at various magnifications; (d) CV curves of NiCo-10 and Ni-10 at 2 mV s^{-1}; (e) GCD curves of NiCo-10 and Ni-10 at 1 A g^{-1}.

Compared with NiCo-10, the main peaks of Ni-10 become wider and the location of some peaks begin to shift, probably attributing to the absence of cobalt ions in the reaction. Besides, the 1D SL structure can't be observed in the FESEM figures. Even so, we still compared electrochemical performance of NiCo-10 and Ni-10. The larger closed area and longer discharge time demonstrates the enhanced effect of Co doped into NiCo-10 composites. Different from NiCo-10, the obvious variation of peaks location in the CV curves of Ni-10 may have a close relationship with the polarization of electrode materials.

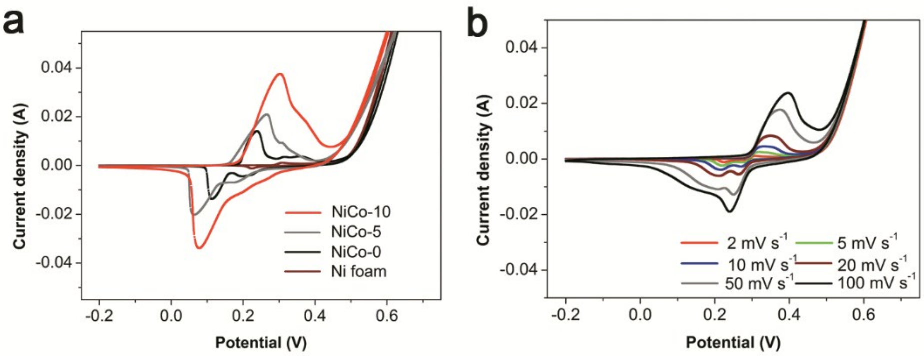

Fig. S11 (a) CV curves of NiCo-0, NiCo-5, NiCo-10 and pristine Ni foam at 2 mV s^{-1}. All these electrodes have an area of 1 cm^2. (b) CV curves of 1 cm^2 Ni foam electrodes at various scanning rates.

In Fig. S11, compared with CV curves of NiCo-0, NiCo-5 and NiCo-10 electrodes, pristine Ni foam possesses an extremely small closed area. Even at 100 mV s^{-1}, the peak current of pristine Ni doesn't exceed 0.03 A. Thus, the capacitance contribution of Ni foam in 3 M KOH electrolyte can be ignored.

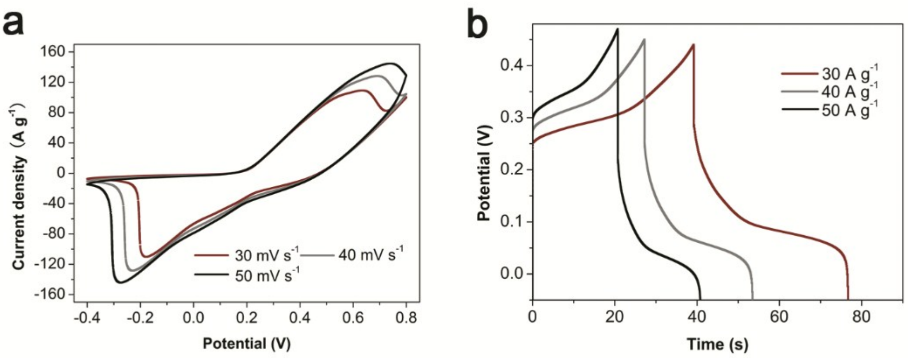

Fig. S12 (a) CV curves of NiCo-10 at high scanning rates; (b) GCD curves of NiCo-10 at high current densities.

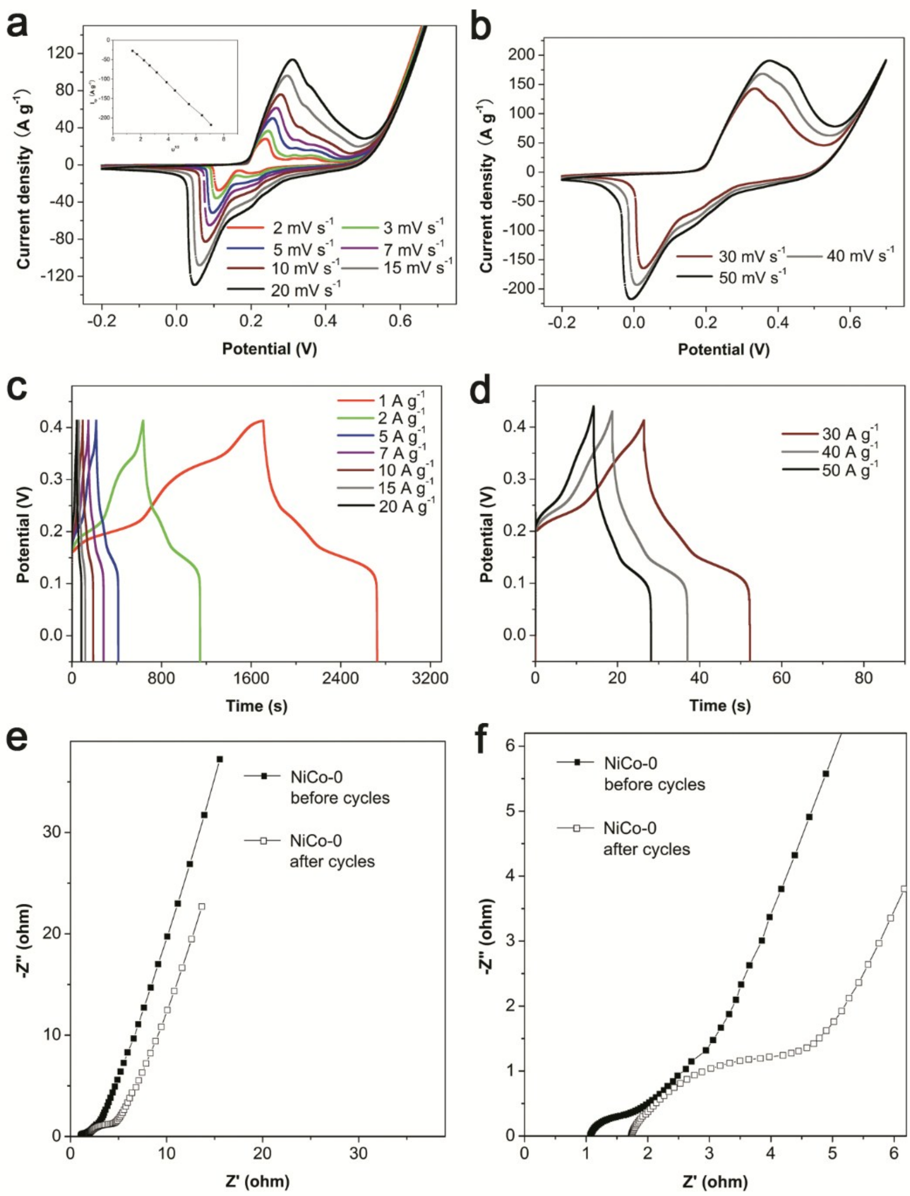

Fig. S13 (a and b) CV curves of NiCo-0 at various scanning rates and corresponding I_{rp}- $\upsilon^{1/2}$ plot in the inset of Fig. S13a; (c and d) GCD curves of NiCo-0 at low and high current densities; (e) EIS spectra of NiCo-5 before and after cycles; (f) Magnification of EIS spectra at high-frequency area.

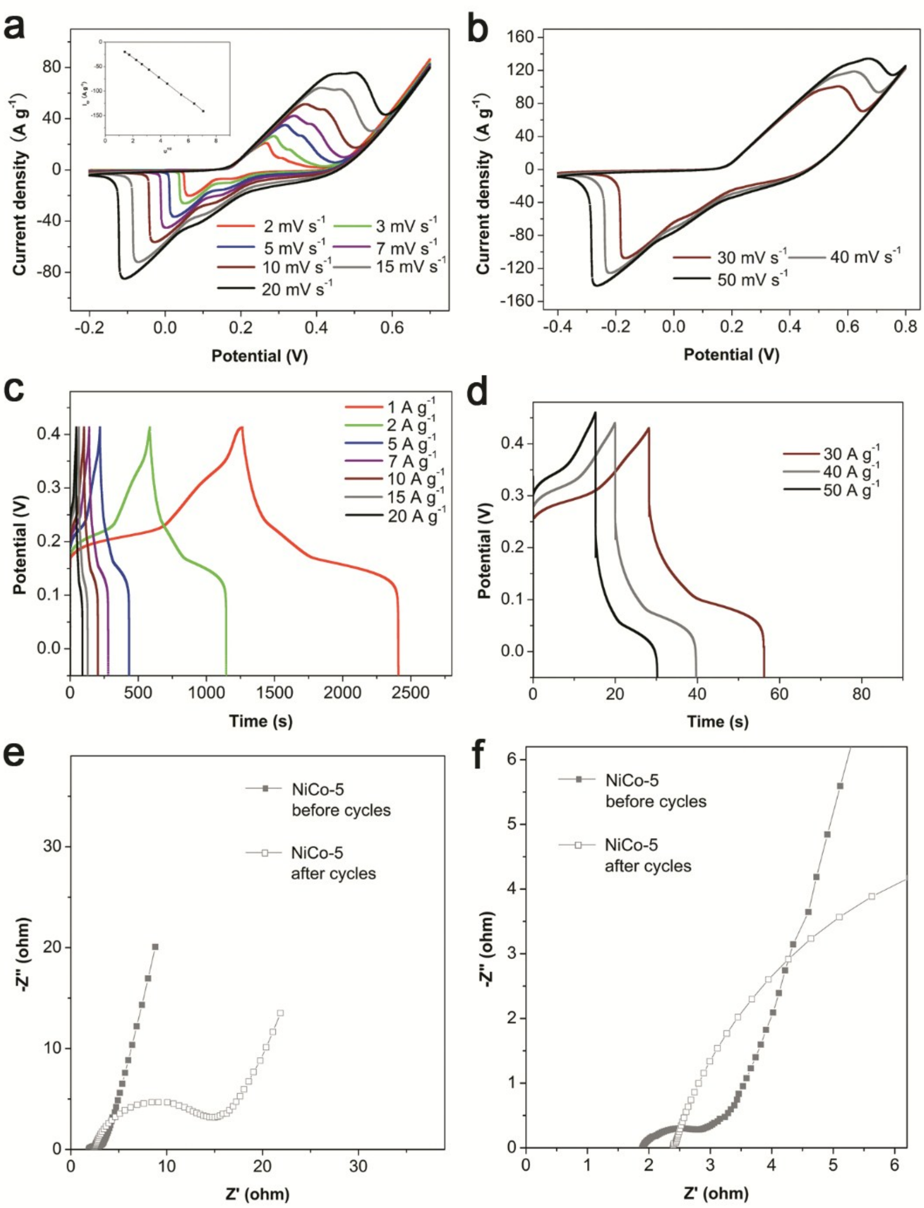

Fig. S14 (a and b) CV curves of NiCo-5 at various scanning rates and corresponding I_{rp}- $\upsilon^{1/2}$ plot in the inset of Fig. S14a; (c and d) GCD curves of NiCo-5 at low and high current densities; (e) EIS spectra of NiCo-5 before and after cycles; (f) Magnification of EIS spectra at high-frequency area.

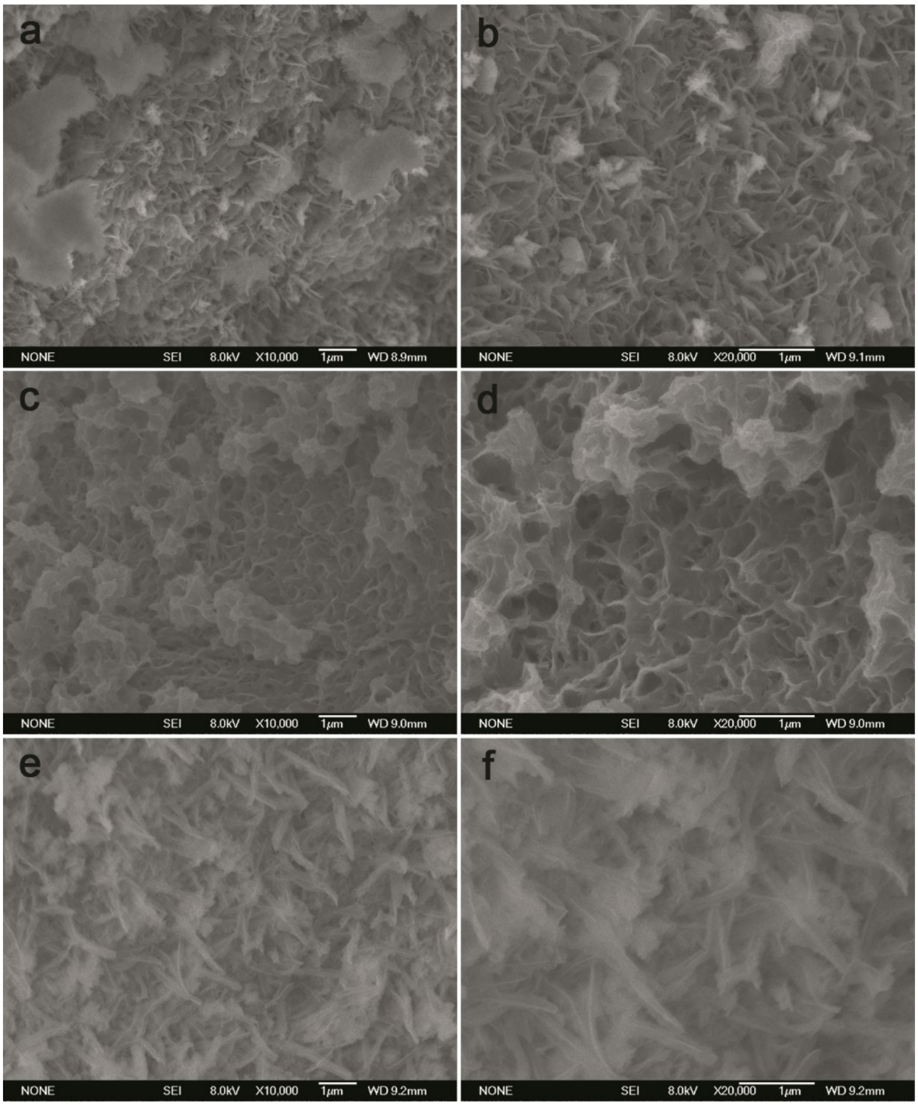

Fig. S15 (a and b) FESEM figures of NiCo-0 after cycles at various magnifications; (c and d) FESEM figures of NiCo-5 after cycles at various magnifications; (e and f) FESEM figures of NiCo-10 after cycles at various magnifications.

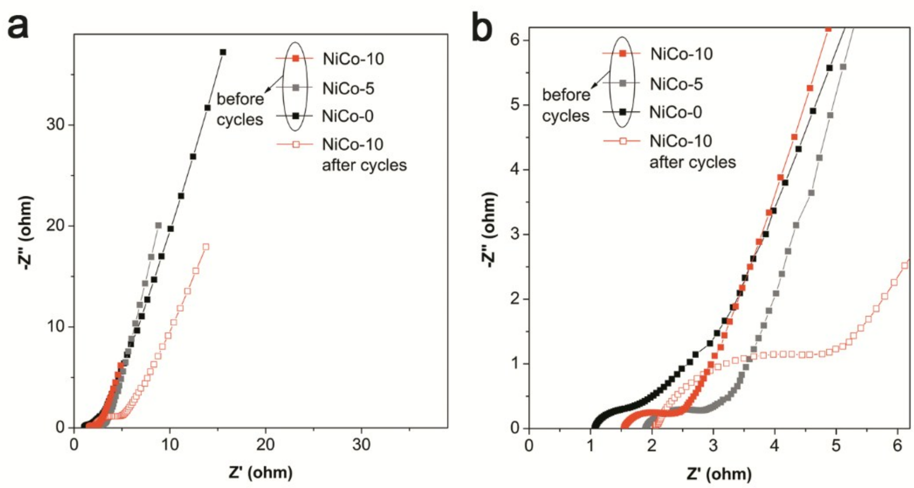

Fig. S16 (a) EIS spectra of NiCo-0, NiCo-5 and NiCo-10 before cycles and NiCo-10 after cycles in a frequency range from 0.01 to 100000 Hz; (b) Magnification of EIS spectra with a range from 0 to 4.2 ohm for Z' value.

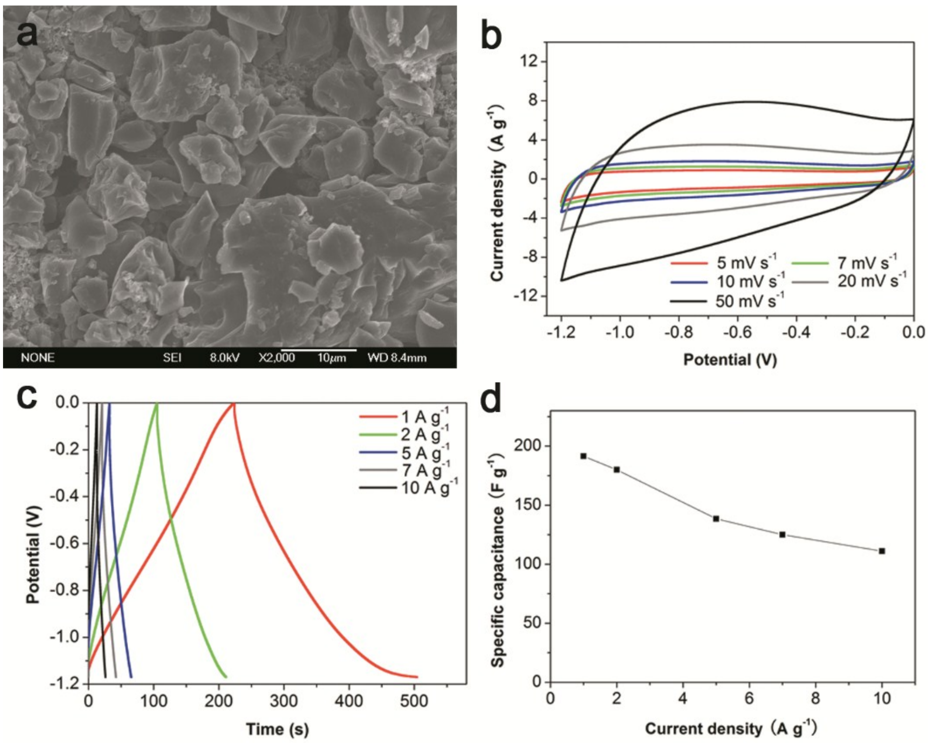

Fig. S17 (a) FESEM figure of AC (YEC-8A) electrode; (b) CV curves of AC electrode at different scanning rates from -1.2 to 0 V; (c) GCD curves of AC electrode at different current densities; (d) Specific capacitances of AC electrodes at various current densities.

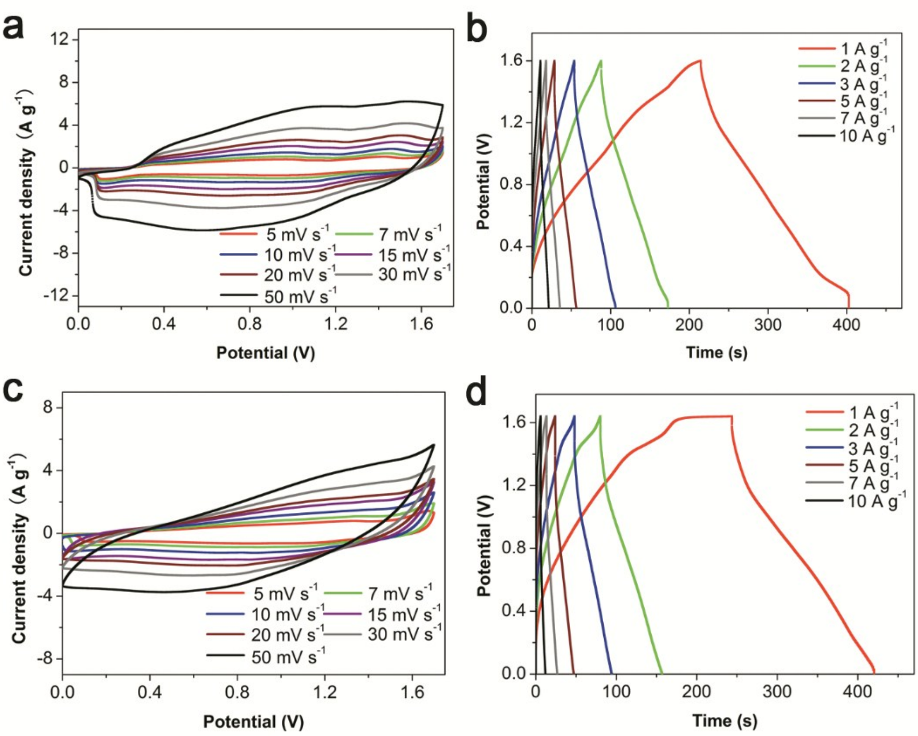

Fig. S18 (a) CV curves of NiCo-0//AC ASC at different scanning rates from 0 to 1.7 V based on a total loading mass of 3.6 mg; (b) GCD curves of NiCo-0//AC ASC at different current densities from 0 to 1.6 V; (c) CV curves of NiCo-5//AC ASC at different scanning rates from 0 to 1.7 V based on a total loading mass of 6.1 mg; (d) GCD curves of NiCo-5//AC ASC at different current densities from 0 to 1.64 V.

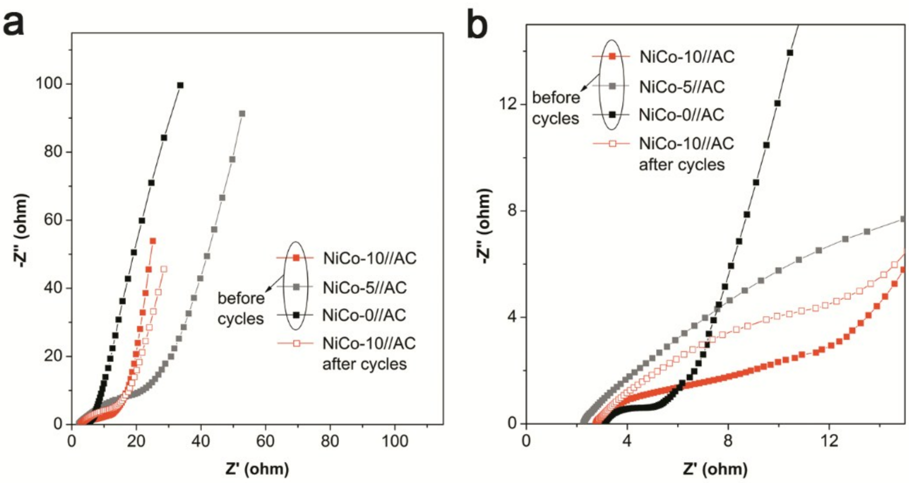

Fig. S19 (a) EIS spectra of NiCo-0//AC, NiCo-5//AC and NiCo-10//AC before cycles and NiCo-10//AC after cycles; (b) Magnification of EIS spectra at high-frequency area.

References

1. K. Wang, C. J. Zhao, S. D. Min and X. Z. Qian, *Electrochim. Acta*, 2015, **165**, 314-322.
2. T. W. Lin, C. S. Dai and K. C. Hung, *Sci. Rep.*, 2014, **4**,7274.
3. X. B. Wang, J. J. Hu, W. D. Liu, G. Y. Wang, J. An and J. S. Lian, *J. Mater. Chem. A,* 2015, **3**, 23333-23344.